Supplementary Information

Catalytic *in vivo* Protein Knockdown by Small Molecule PROTACs

Daniel P. Bondeson[1†], Alina Mares[5†], Ian E.D. Smith[5†], Eunhwa Ko[1], Sebastien Campos[5], Afjal H. Miah[5], Katie E. Mulholland[5], Natasha Routly[5], Dennis L. Buckley[1], Jeffrey L. Gustafson[1], Nico Zinn[6], Paola Grandi[6], Satoko Shimamura[6], Giovanna Bergamini[6], Maria Faelth-Savitski[6], Marcus Bantscheff[6], Carly Cox[1], Deborah A. Gordon[7], Ryan R. Willard[7], John J. Flanagan[7], Linda N Casillas[8], Bartholomew J Votta[8], Willem den Besten[4], Kristoffer Famm[5], Laurens Kruidenier[5], Paul S. Carter[5], John D. Harling[5], Ian Churcher[5*], Craig M. Crews[1,2,3*]

[†*]These Authors contributed equally to this work

[1]Department of Molecular, Cellular and Developmental Biology, Yale University, New Haven, CT.

[2]Department of Chemistry, Yale University, New Haven, CT.

[3]Department of Pharmacology, Yale University, New Haven, CT.

[4]Division of Biology & Biological Engineering, California Institute of Technology, Pasadena, CA.

[5]GSK Medicines Research Centre, Gunnels Wood Road, Stevenage, UK SG1 2NY.

[6]Cellzome, a GSK company, Meyerhofstr. 1, 69117 Heidelberg, Germany.

[7]Arvinas, Inc., New Haven, CT.

[8] Pattern Recognition Receptor Discovery Performance Unit, GlaxoSmithKline, Collegeville, PA

Supplementary Results
Supplementary Figures

Supplementary Figure 1. PROTAC parent ligand structures

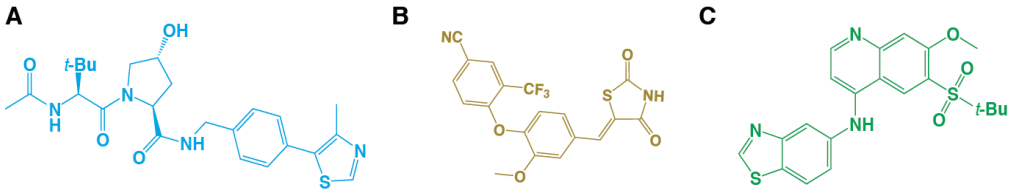

A) VHL Ligand
B) ERRα Ligand (Compound 29 in Reference 21)
C) RIPK2 ligand

Supplementary Figure 2: The parent Compound 29 does not degrade ERRα

3T3-L1 cells were treated for 16 hours with the indicated concentrations of Compound 29, the parent ligand for PROTAC_ERRα, followed by harvesting and western blot as described in Materials and Methods. Quantification was performed by densitometry, and values are normalized to tubulin and the vehicle control. Values are representative of at least two experiments.

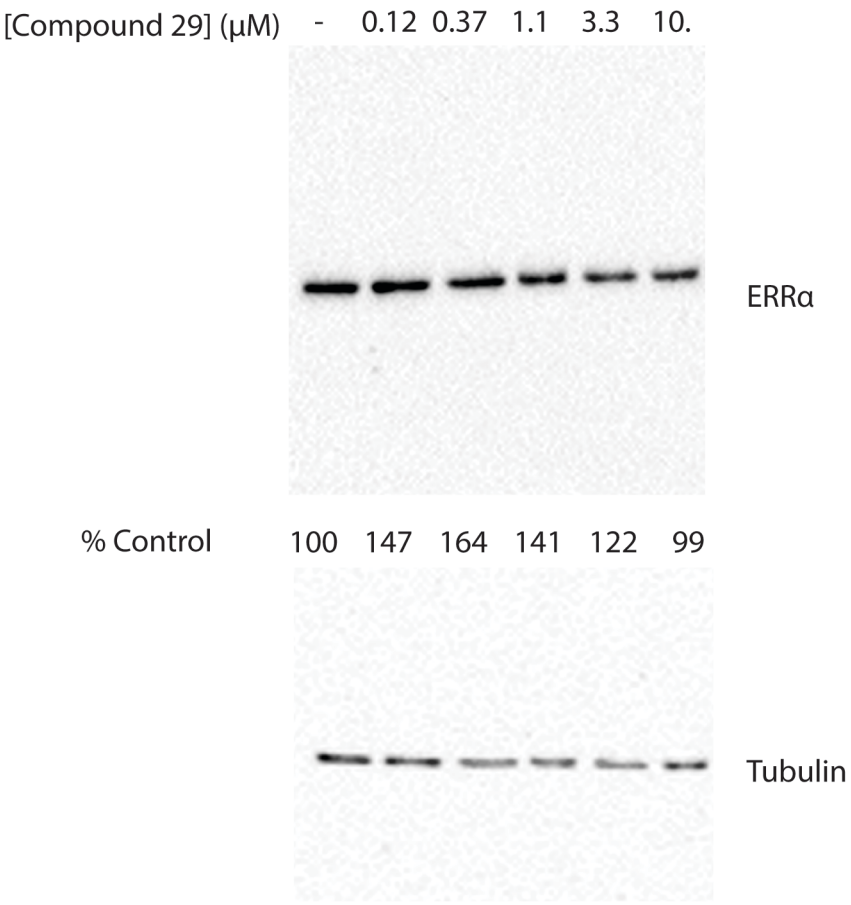

Supplementary Figure 3. Effect of linker on RIPK2 degradation efficiency.

The linker for PROTAC_RIPK2, presented in the main text, was based on a previous generation of RIPK2 PROTACs utilizing the tyrosine kinase inhibitor vandetanib. The Structure-Activity Relationship for different linkers showed that the three PEG linker afforded maximal degradation. Based on these observations, the optimal linker (entry 2) was used in PROTAC_RIPK2.

Targeting Ligand	Linker	DC_{50}
Vandetanib 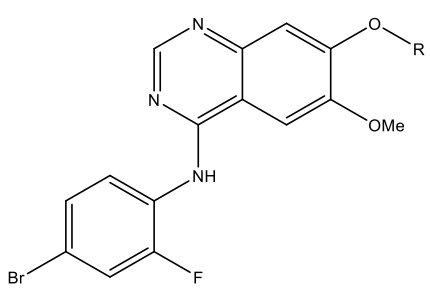	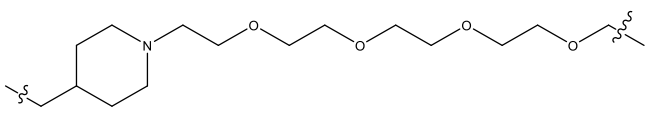	Weak effect at 10 μM
	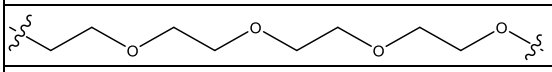	0.8 μM
	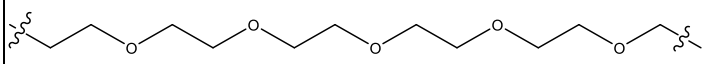	No effect up to 3µM
	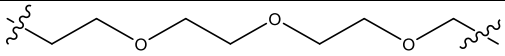	2 μM

Supplementary Figure 4. Inhibition of HIF1a peptide binding to VHL complex by

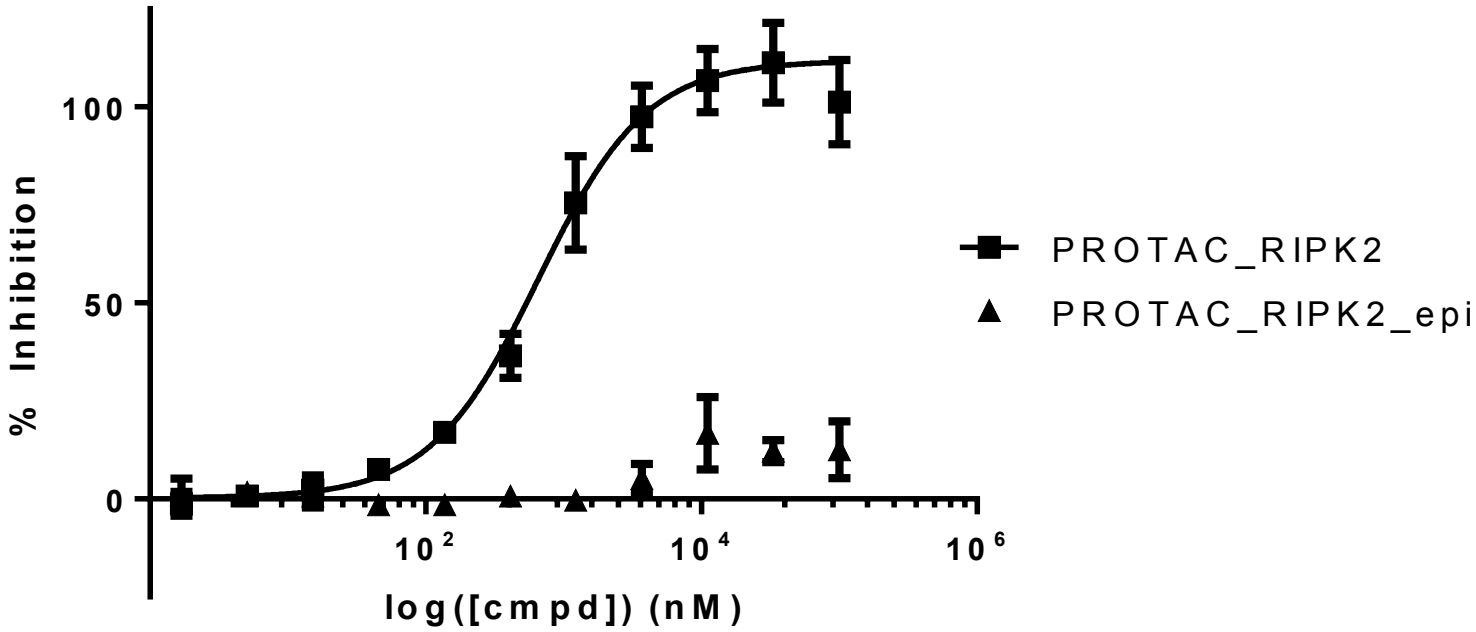

PROTACs

In a competitive fluorescence polarization experiment, a labeled HIF1α probe was in competition with either PROTAC_RIPK2 or PROTAC_RIPK2_epi. The fit sigmoid for PROTAC_RIPK2 demonstrates an IC_{50} of 656 nM. Data shown are mean ± SD of at least 4 experiments.

Supplementary Figure 5. Effect of PROTAC_RIPK2 and PROTAC_ERRα on ODD-luciferase

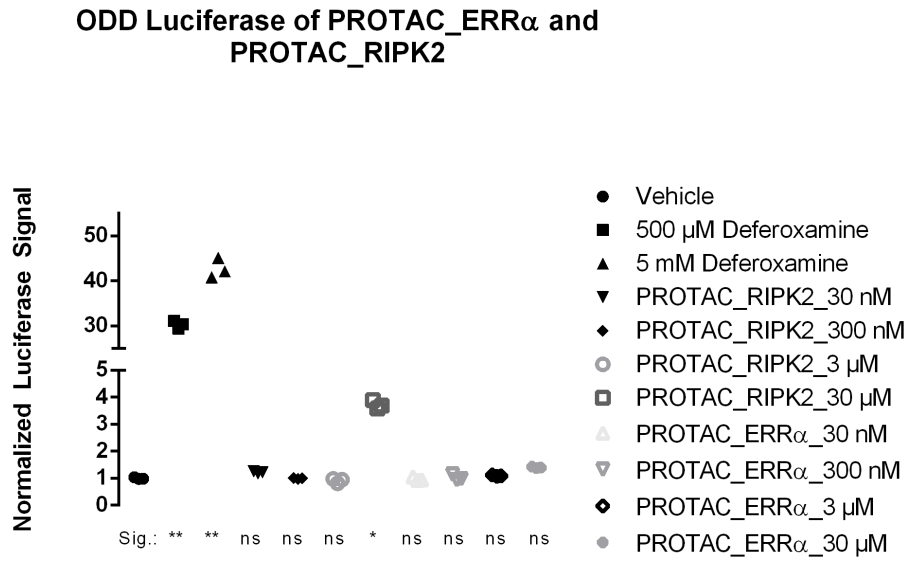

SH-SY5Y cells expressing luciferase fused to the first Oxygen Dependent Degradation (ODD) of HIF1α were treated in triplicate for 16 hours with the indicated compounds. The iron chelator Deferoxamine (Sigma) was used as a positive control for hypoxic response. Luciferase levels were analyzed in whole cell extracts. ** $p<0.0001$, *$p<0.001$, ns: not significant by an ANOVA test compare to vehicle.

Supplementary Figure 6. Full blots of *in cellula* protein degradation.

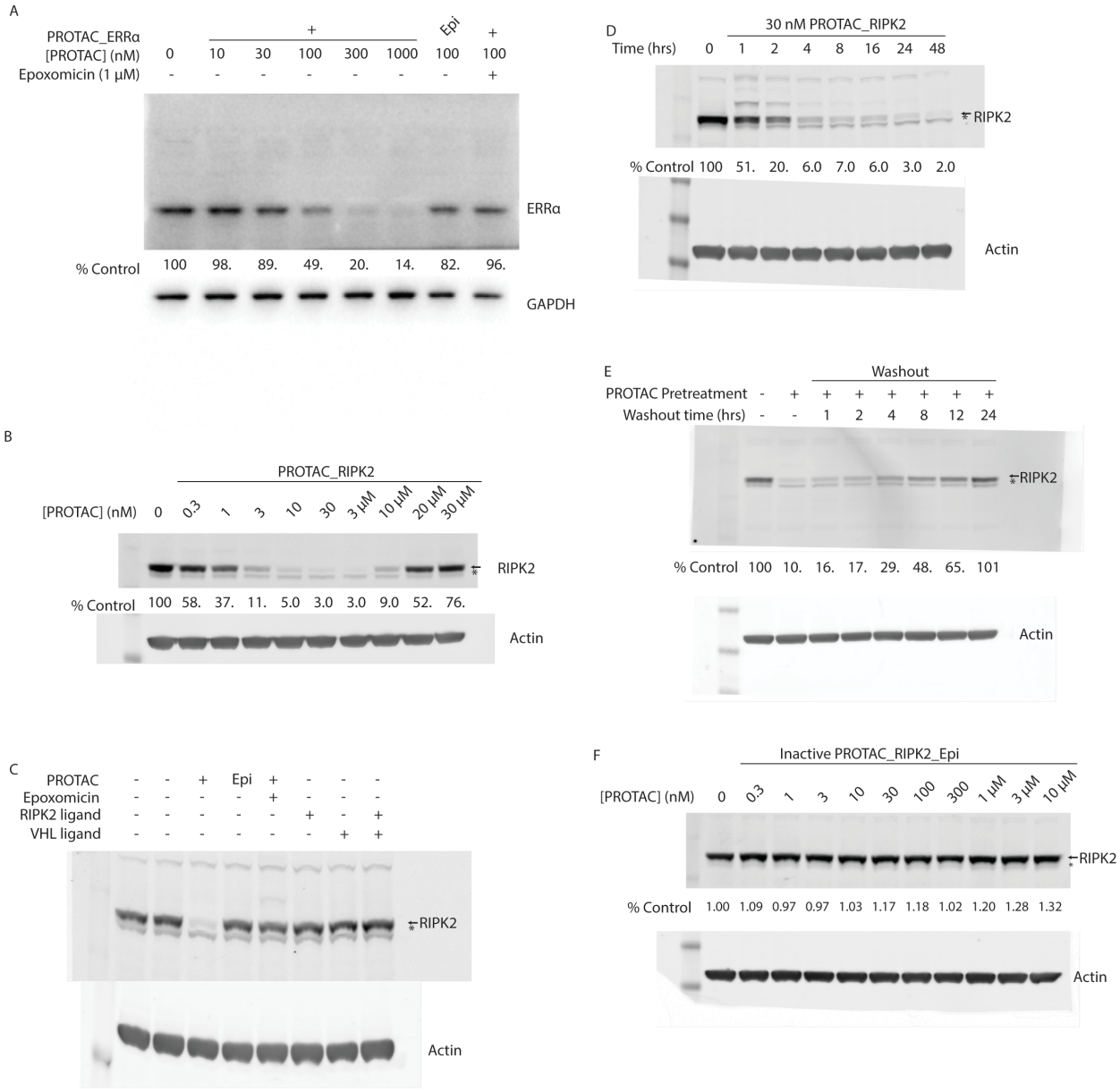

Supplementary Figure 7. PROTAC_RIPK2 is not toxic to cells

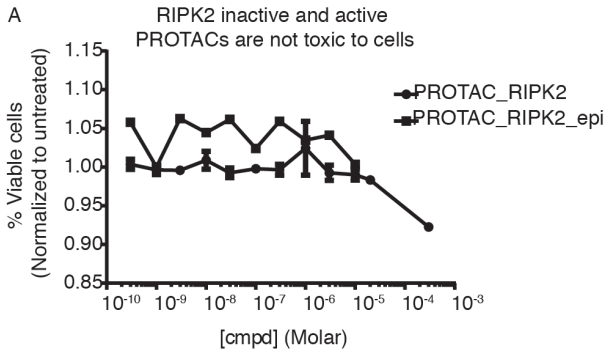

(A) Cell viability with RIPK2 PROTACs. THP-1 cells were treated with the indicated concentrations of PROTAC_RIPK2 or PROTAC_RIPK2_epi for 16 hours, followed by a Trypan Blue assay to determine cell viability. Error bars represent mean and S.D.

Supplementary Figure 8. Demonstration of a PROTAC-mediated ternary complex between RIPK2 and VHL

Immunoaffinity enrichment of endogenous VHL from THP-1 cell extract in the presence of RIPK2 inhibitor, PROTAC_RIPK2 and PROTAC_RIPK2_epi. Immunoblotting demonstrates enrichment of VHL (bottom) using an anti-VHL antibody as compared to IgG control. In the presence of various concentrations of PROTAC_RIPK2 but not with PROTAC_RIPK2_epi and RIPK2-binding ligand, RIPK2 is selectively co-precipitated (top). Shown are replicate n=1 and replicate n=2.

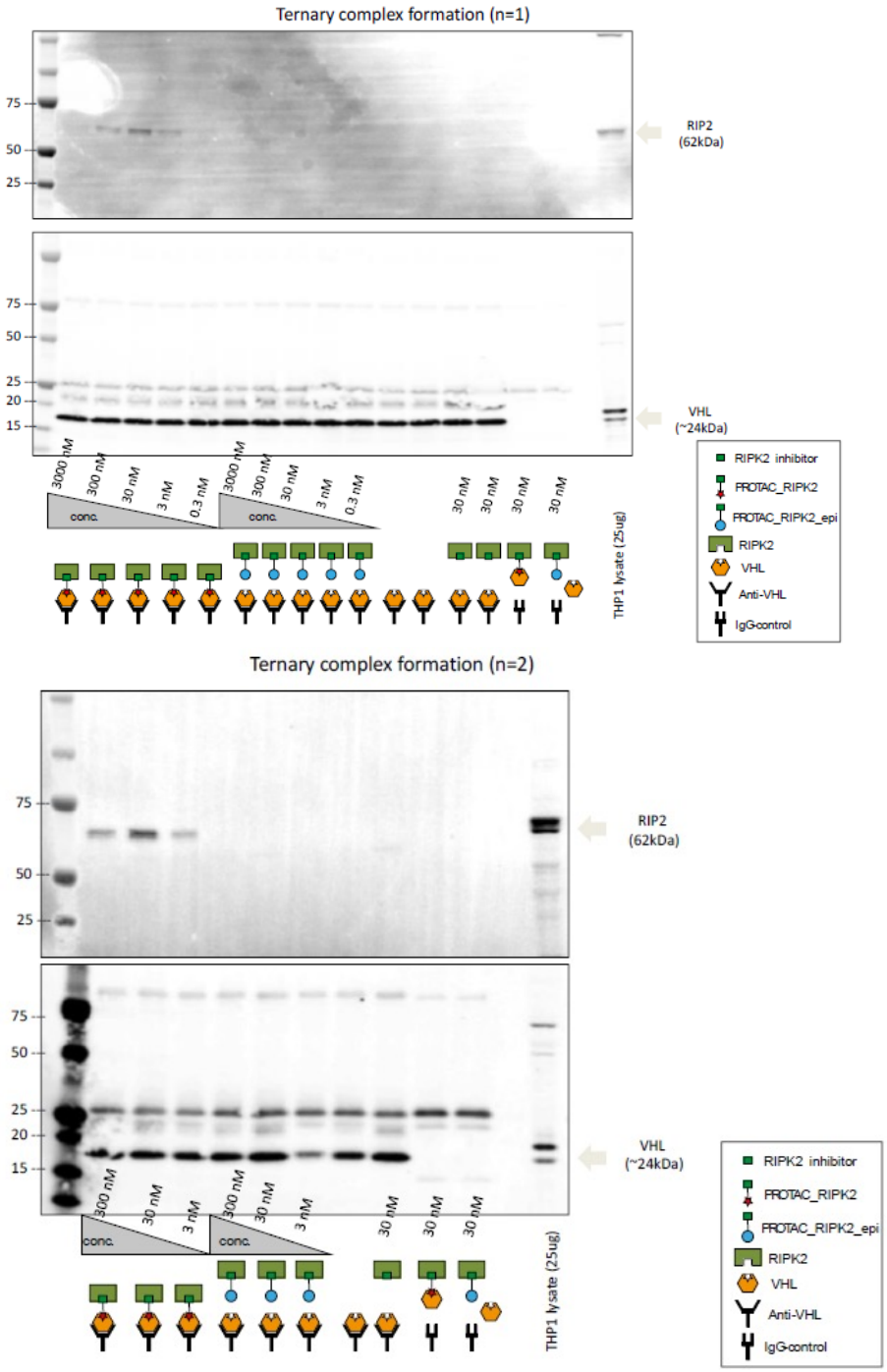

Supplementary Figure 9A. Kinome specificity of RIPK2 ligand

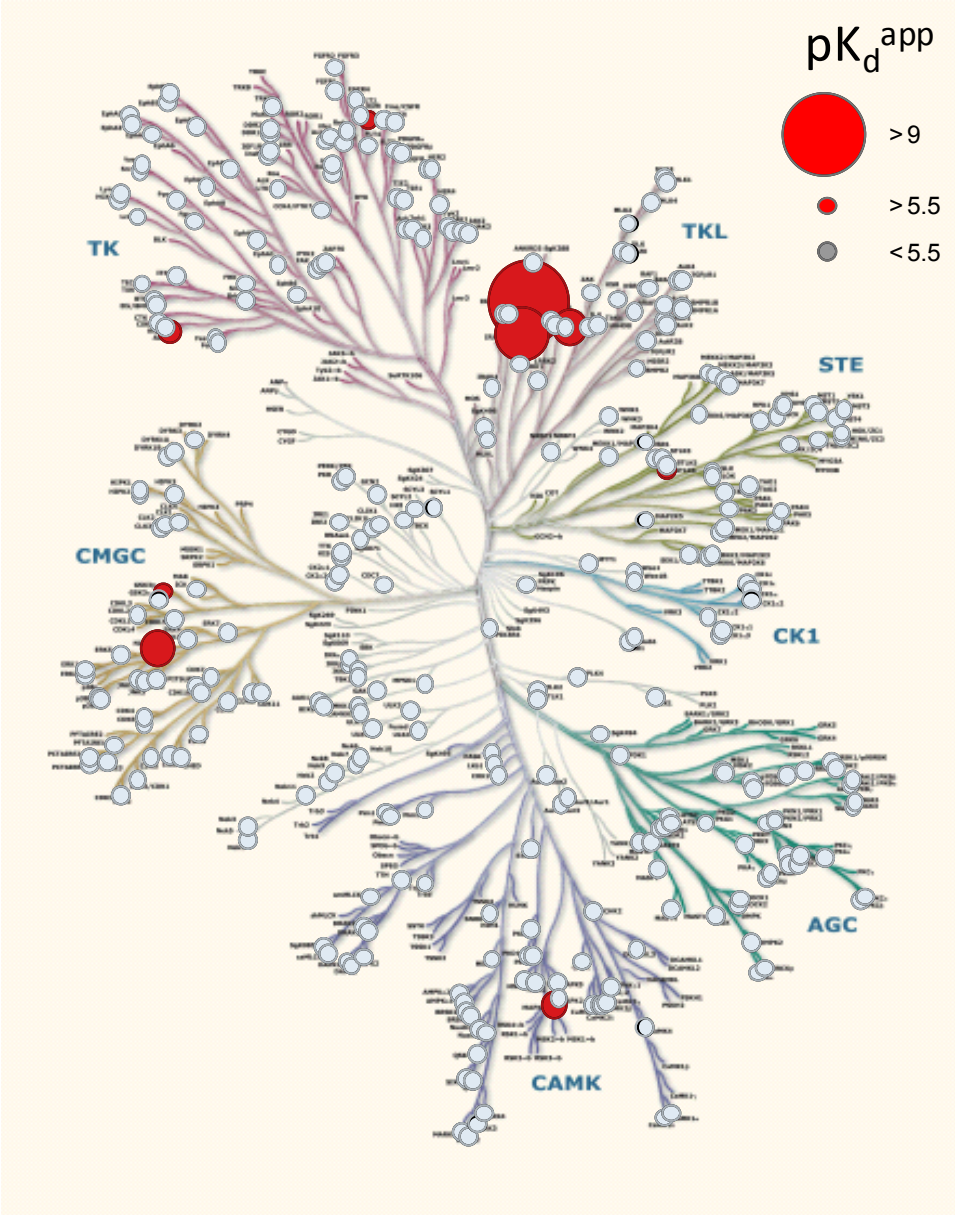

The specificity of the RIPK2 ligand was profiled against 371 kinases by KinoBead profiling (average of 2 determinations).

Supplementary Figure 9B. Summary of significant activities from kinobead profiling of RIPK2-Ligand, PROTAC_RIPK2 and PROTAC_RIPK2_epi

Protein	pK_D^{app}		
	RIPK2-Ligand	PROTAC RIPK2	PROTAC RIPK2_epi
RIPK2	9.3	8.6	8.5
RIPK3	7.7	6.6	6.7
NLK	6.7	<5.5	<5.5
ABL1/BCR-ABL	6.5	6.2	6.1
TESK2	6.7	6.1	6.3
TGFBR2	6.2	<5.5	<5.5
MAPKAPK3	6.1	<5.5	<5.5

The PROTACS interact with similar kinases to the parent ligand though absolute pK_D^{app} values (mean of n=2) are slightly lower. Both PROTACs show almost identical profiles to each other.

Supplementary Figure 10A. RIPK2 Proteomics time and concentration

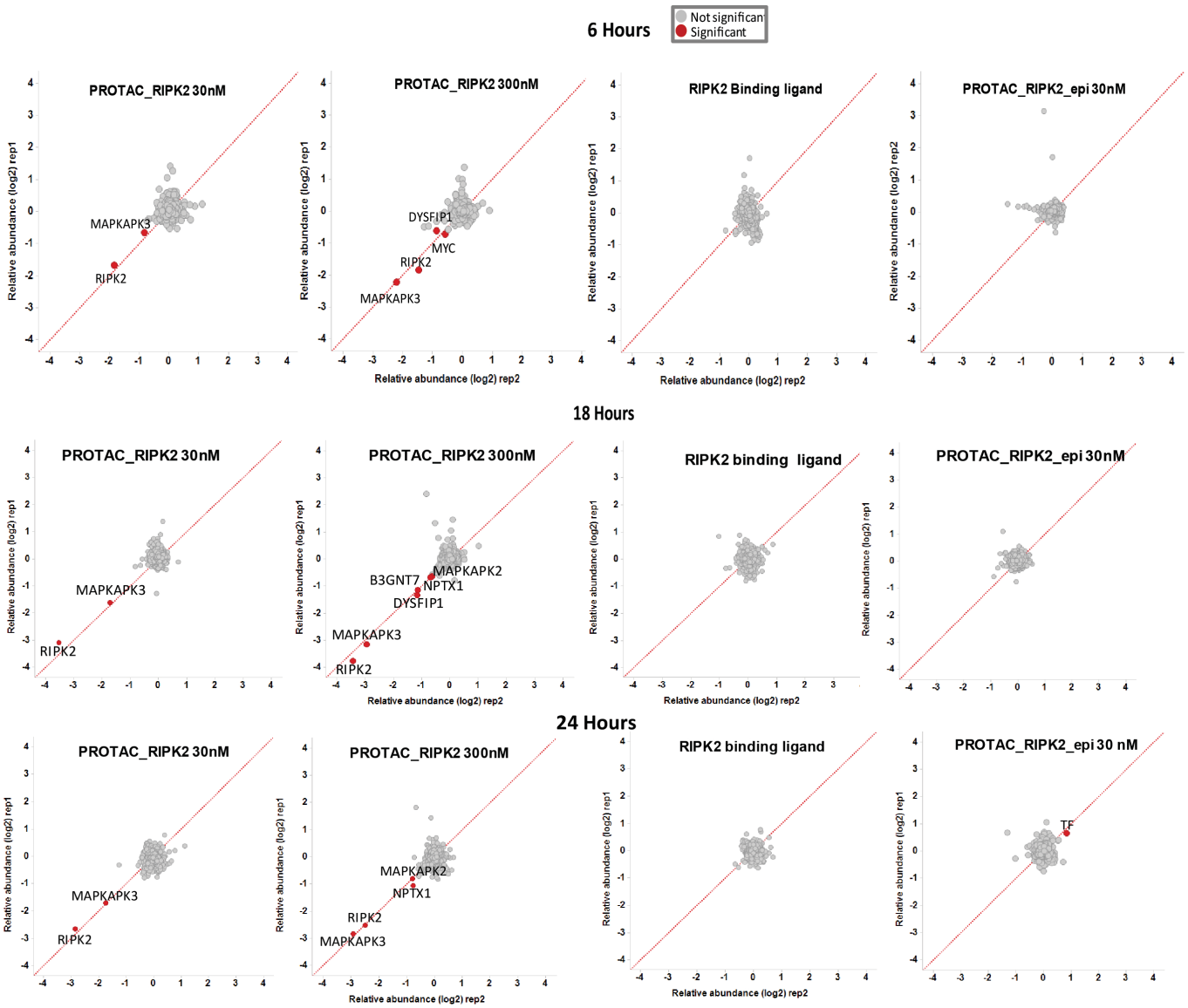

dependence

Proteomic analysis of protein abundances in response to treatment of THP1 cells with the indicated agent at the indicated time. Scatter plots depicting relative abundances of detected proteins (circles) from THP-1 cells incubated for 6 h with 30 and 300 nM PROTAC_RIPK2, 30 nM Protac_RIPK2_epi and RIPK2-binding ligand compared to vehicle treated samples. . Proteins significantly ($p<0.05$) regulated in the two biological replicate experiments are indicated in red. Relative abundance is plotted replicate 1 vs replicate 2 on a Log2 scale.

Supplementary Figure 10B. ERRα Proteomics time and concentration

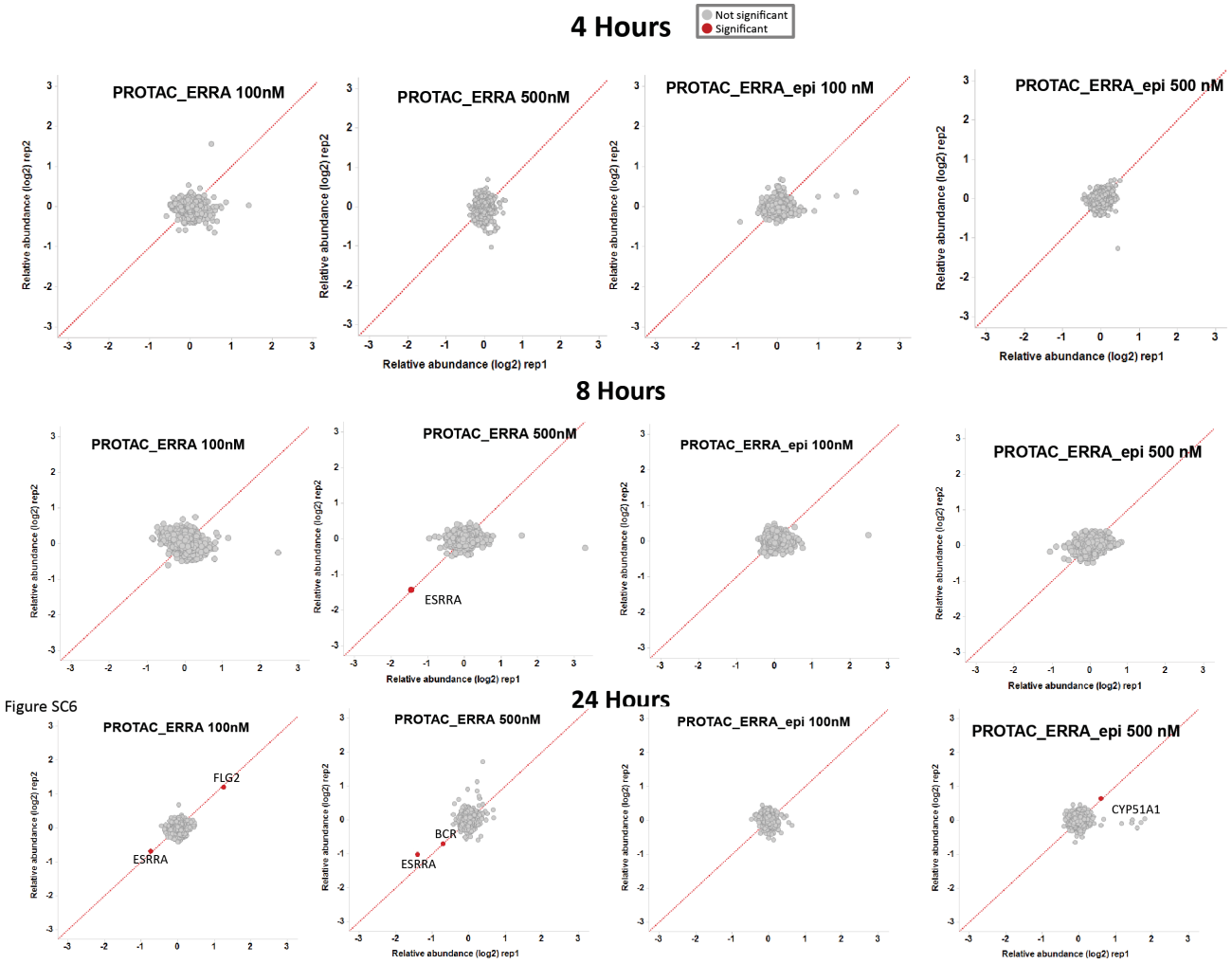

Figure SC6

dependence

Proteomic analysis of protein abundances in response to treatment of MCF-7 cells with the indicated agent at the indicated time. Scatter plots depicting relative abundances of detected proteins (circles) from MCF-7 cells incubated for 4 h with 100 and 500 nM PROTAC_ ERRα and ERRα_epi compared to vehicle treated samples. Proteins significantly ($p<0.05$) regulated in the two biological replicate experiments are indicated in red. Relative abundance is plotted replicate 1 vs replicate 2 on a Log2 scale.

Tables

Supplementary Table 1**:** Relative abundance of proteins immunoprecipitated with the active or inactive VHL ligands. This data table is graphically represented in Figure 3A. See file “Table S1 Bondeson et al”.

Supplementary Table 2**:** Results summary for ternary complex formation. This data table is graphically represented in Figure 3C. See file “Table S4 Bondeson et al”

Supplementary Table 3**:** Proteomic analysis of RIPK2 phosphorylation sites. LC/MS/MS analysis of RIPK2 recombinant protein after incubation in kinase buffer with or without ATP. See file “Table S3 Bondeson et al”.

Supplementary Table 4**:** Results summary for Kinobead competition binding experiments. This data table is graphically represented in Supplementary Figure 8. See file “Table S2 Bondeson et al”.

Supplementary Table 5: Results summary for expression proteomics. This data table is graphically represented in Figure 4 and Supplementary Figure 9. See file “Table S5 Bondeson et al”.